Hindawi Publishing Corporation
Journal of Nanomaterials
Volume 2014, Article ID 401697, 6 pages
http://dx.doi.org/10.1155/2014/401697

Research Article

Preparation of $BiVO_4$-Graphene Nanocomposites and Their Photocatalytic Activity

Xuan Xu,[1,2] Qiulin Zou,[1] Yunsong Yuan,[1] Fangying Ji,[1] Zihong Fan,[3] and Bi Zhou[1]

[1] *Key Laboratory of Three Gorges Reservoir Region's Eco-Environment, Ministry of Education, Chongqing University, Chongqing 400045, China*
[2] *National Centre for International Research of Low-carbon and Green Buildings, Chongqing University, Chongqing 400045, China*
[3] *School of Environmental and Biological Engineering, Chongqing Technology and Business University, Chongqing 400067, China*

Correspondence should be addressed to Xuan Xu; xuxuan@cqu.edu.cn

Received 24 January 2014; Accepted 31 March 2014; Published 12 May 2014

Academic Editor: Shijun Liao

We prepared $BiVO_4$-graphene nanocomposites by using a facile single-step method and characterized the material by x-ray diffraction, scanning electron microscopy, Fourier-transform infrared spectroscopy, ultraviolet-visible diffuse-reflection spectroscopy, and three-dimensional fluorescence spectroscopy. The results show that graphene oxide in the catalyst was thoroughly reduced. The $BiVO_4$ is densely dispersed on the graphene sheets, which facilitates the transport of electrons photogenerated in $BiVO_4$, thereby leading to an efficient separation of photogenerated carriers in the coupled graphene-nanocomposite system. For degradation of rhodamine B dye under visible-light irradiation, the photocatalytic activity of the synthesized nanocomposites was over ~20% faster than for pure $BiVO_4$ catalyst. To study the contribution of electrons and holes in the degradation reaction, silver nitrate and potassium sodium tartrate were added to the $BiVO_4$-graphene photocatalytic reaction system as electron-trapping agent and hole-trapping agent, respectively. The results show that holes play the main role in the degradation of rhodamine B.

1. Introduction

In recent years, nanometer photocatalysis technology has attracted widespread interest because of its potential applications in water splitting and environmental remediation [1, 2]. To prepare high-activity photocatalysts, researchers have made every effort to prepare new types of photocatalysts such as TiO_2 [3], Bi_2WO_6 [4], ZnO [5], and $BiVO_4$ [6]. To date, from among the various photocatalysts, TiO_2 has been investigated most extensively because it is nontoxic, chemically inert, and photostable. However, its application is limited by its wide band gap (3.2 eV), which means that ultraviolet (UV) irradiation is required to activate photocatalysis. This is problematic because UV accounts for only about 4% of the entire terrestrial solar spectrum, whereas visible light accounts for about 45% of this spectrum [7, 8]. Therefore, much research has recently gone into developing photocatalysts that can be activated by visible light.

For many years, $BiVO_4$ was widely used to produce yellow paint. However, recent studies have found that monoclinic $BiVO_4$, which has a band gap of 2.4 eV, is an ideal visible-light photocatalytic material for recycling polluted water. In addition, it also has the advantages of low cost, environmental friendliness, and high stability against photocorrosion [9, 10]. However, the conduction band of $BiVO_4$ is just slightly above 0 eV, which would make it hard for O_2 to capture electrons photoexcited by visible light [11]. In addition, in the photocatalytic reaction, the oxidation-reduction reaction competes with electron-hole recombination [12]. Eventually, the electron-hole recombination rate increases. Finally, the low photocatalytic activity of pure $BiVO_4$ restricts its wide application for photocatalytic degradation of organic contaminants [13–16].

As a new type of two-dimensional carbon material, graphene possesses a number of excellent intrinsic properties. For example, its band gap is almost zero and it has high electrical conductivity, high specific surface area (2630 m^2/g), and high carrier mobility (200 000 cm^2/V) [17–21]. In searching for new strategies to promote the photoactivity

of semiconductors, graphene-based nanocomposites have recently emerged as the most prominent candidates. Notably, the abundance of delocalized electrons in the π-conjugated electronic structure of graphene endows it with outstanding electronic conductivity. In coupled graphene-nanocomposite systems, this high conductivity facilitates the transport of charges photogenerated in the attached semiconductors, thereby leading to efficient separation of photogenerated charge carriers [14, 22, 23].

Graphene oxide is an important derivative of graphene. Its structure and properties are similar to those of graphene and it is easily produced and commonly used as a precursor for grapheme [13–15, 24].

Inspired by these concepts, we report herein the design and synthesis of graphene-based nanocomposites, using $BiVO_4$-graphene nanocomposites as an example, with the goal of achieving highly efficient photocatalytic properties driven by visible light.

2. Experiment

2.1. Experimental Materials. The following analytically pure chemicals were used: graphite powder (≥99.85%, Shanghai HuaYi Company), sodium nitrate ($NaNO_3$, Chengdu Kelon Chemical Reagent Company), potassium permanganate ($KMnO_4$, Chongqing Chuandong Chemical Company), sulfuric acid (H_2SO_4, Chongqing Chuandong Chemical Company), hydrogen peroxide (H_2O_2, Chongqing Chuandong Chemical Company), bismuth nitrate [$Bi(NO_3)_3{\cdot}5H_2O$, Chengdu Kelon Chemical Reagent Company], sodium vanadate ($Na_3VO_4{\cdot}12H_2O$, Sinopharm Chemical Reagent Company), hexadecyl trimethyl ammonium bromide ($C_{19}H_{42}BrN$, Chengdu Kelon Chemical Reagent Company), sodium chloride (NaCl, Chongqing Chuandong Chemical Company), hydrochloric acid (HCl, Chongqing Chuandong Chemical Company), cyclohexane (C_6H_{12}, Chongqing Chuandong Chemical Company), glucose ($C_6H_{12}O_6$, Chongqing Boyi Chemical Company), and 25% of ammonia solution ($NH_3{\cdot}H_2O$, Chongqing Chuandong Chemical Company).

2.2. Synthesis of $BiVO_4$. Typically, the synthesis of $BiVO_4$ proceeds as follows: 4.8 mmol hexadecyl trimethyl ammonium bromide and 1.6 mmol $Bi(NO_3)_3{\cdot}5H_2O$ are added in that order to distilled water (40 mL). Next, 1.6 mmol $Na_3VO_4{\cdot}12H_2O$ in 40 mL distilled water is added to the above solution. After vigorous stirring for 10 min, the mixture is transferred into a 50 mL Teflon-lined autoclave and then sealed and heated at 120°C for 10 h. The system is allowed to naturally cool down to room temperature. The final product was collected by centrifuging the mixture. It was then washed with distilled water six times and then dried under vacuum overnight at 60°C for 12 h.

2.3. Synthesis of $BiVO_4$-Graphene. Graphene oxide was synthesized according to the modified Hummers method [13, 24]. To synthesize $BiVO_4$-graphene, 200 mg $BiVO_4$, 2 mg of graphene sheets, and 60 mL cyclohexane were added to a 100 mL beaker, and then the mixture was sonicated in an ultrasonic bath for about 30 min. The precipitate was filtered and dried in a vacuum oven at 40°C for 12 h [13]. The resulting dark-green powder was collected for further characterization.

2.4. Characterization. Powder X-ray diffraction (XRD) spectra were acquired with a Rigaku D/Max-rB diffractometer with Cu Kα radiation. The 2θ scanning angle ranged from 10° to 70°. Scanning electron microscopy (SEM) images were acquired with a Zeiss AURIGA FIB (EDT = 3 kV; WD = 5.2 nm). Fourier-transform infrared (FT-IR) spectra were recorded on a Shimadzu IR Prestige-1 spectrometer by using the KBr-pellet technique. UV-visible diffuse-reflectance spectroscopy (UV-Vis DRS) was done with a Hitachi U-3010 UV-Vis spectrometer. Three-dimensional (3D) fluorescence spectra were obtained with a Hitachi F-7000 fluorescence spectrophotometer with a 150 W Xe lamp as excitation source. The EX and EM slits were both set at 5 nm, and the photomultiplier-tube voltage was 400 V.

2.5. Photocatalytic-Activity Measurement. The photocatalytic activity of the samples was determined by the degradation of rhodamine B (RhB) under visible-light irradiation. A 450 W high-pressure mercury lamp was used as the visible-light irradiation source. For the experiments, 0.15 g of catalyst was first added to 400 mL of 5 mg/L RhB aqueous solution. Before irradiation, the reaction mixture was stirred for 30 min in the dark to reach adsorption-desorption equilibrium between dye and catalyst. After 2 h sessions of irradiation, 8 mL aliquots were withdrawn and centrifuged to remove essentially all catalysts. The concentration of the remnant dye was spectrophotometrically monitored by measuring the absorbance of solutions at 552 nm during the photodegradation process.

3. Results and Discussion

3.1. X-Ray Diffraction. Figure 1 shows XRD patterns of the pure $BiVO_4$ and $BiVO_4$-graphene. Almost all the diffraction peaks of pure $BiVO_4$ and $BiVO_4$-graphene can be assigned to monoclinic $BiVO_4$ (JCPDS 14-0688), which is the most active photocatalyst under visible-light irradiation [14]. This explains why the photocatalysts remain in a monoclinic structure and why the phase of $BiVO_4$ does not change after adding the graphene-oxide solution. However, no diffraction peak typical of graphite or graphene oxide appears in the XRD pattern of $BiVO_4$-graphene. We attribute this result to the fact that graphene oxide can be thoroughly reduced to graphene, which has no XRD peaks in this range [23].

3.2. SEM. Figure 2 shows SEM images of different samples. The images show clearly that pure $BiVO_4$-particles form a fine structure composed of $BiVO_4$ crystal grains. At the same time, some $BiVO_4$ aggregates and $BiVO_4$-graphene particles appear. $BiVO_4$ and graphene sheets are in close contact, which facilitates the transport of electrons photogenerated in $BiVO_4$, thereby leading to efficient separation of photogenerated carriers in the coupled graphene-nanocomposite

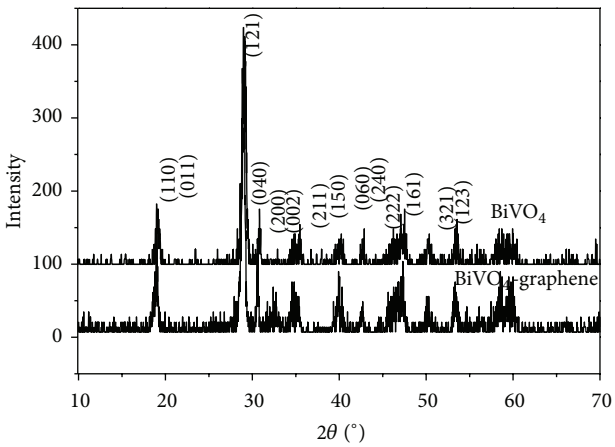

Figure 1: XRD patterns of pure $BiVO_4$ and $BiVO_4$-graphene composites.

system. As a result, we expect this material to have enhanced photocatalytic activity [25].

3.3. FT-IR. Figure 3 shows the Fourier-transform infrared (FTIR) spectra of graphene, graphene oxide, pure $BiVO_4$, and a $BiVO_4$-graphene composite. Graphene oxide exhibits a peak at 1731 cm^{-1} for C=O stretching vibrations. The peaks at 1127 and 1196 cm^{-1} are assigned to phenolic hydroxyl groups. Tertiary C–OH at the edges appear at 1335 cm^{-1} and C–O stretching vibrations of the epoxy groups appear at 1031 and 1051 cm^{-1} [26, 27]. For graphene, the adsorption around 1567 cm^{-1} may be assigned to stretching vibrations of the unoxidized carbon backbone, which suggests that the graphene oxide has been reduced [14]. It is clear that, for graphene, almost all the peaks characteristic of graphene oxide disappear except for C–OH. For $BiVO_4$-graphene and pure $BiVO_4$, the broad absorptions at low frequency (such as 729 cm^{-1}) are attributed to VO_4^{3-} [14]. However, no peak typical of graphite or graphene oxide is observed in the FT-IR spectra of $BiVO_4$-graphene. We attribute this result to the low amount of graphene (1%).

3.4. UV-Vis DRS. Figure 4 shows representative spectra of pure $BiVO_4$ and a $BiVO_4$-graphene composite. It is clear that the absorption spectrum of the $BiVO_4$-graphene nanocomposite is almost the same as that of pure $BiVO_4$. The spectrum of the $BiVO_4$-graphene composite lies above that of pure $BiVO_4$ because of the graphene in the composite. These results illustrate that incorporating graphene could significantly increase the absorption of visible light, meaning that visible light could be better utilized simply by combining graphene with $BiVO_4$.

3.5. PL. Photoluminescence (PL) spectra reflect the migration, transfer, and recombination processes of the electron-hole pairs [28–30]. Figure 5 shows 3D fluorescence spectra of pure $BiVO_4$ and $BiVO_4$-graphene. The plots show that both catalysts have a maximum fluorescence peak near $(\lambda_{ex}, \lambda_{em})$ = (202 nm, 310 nm) and $(\lambda_{ex}, \lambda_{em})$ = (202 nm, 505 nm), which is attributed to the recombination of holes and electrons across the band gap of $BiVO_4$. The $BiVO_4$-graphene composites absorb more weakly than pure $BiVO_4$, which implies that the recombination of photogenerated electrons and holes is much less in the $BiVO_4$-graphene composites.

3.6. Photocatalytic Activity of Catalysts. The photodegradation rates of RhB on $BiVO_4$-graphene and on pure $BiVO_4$ under visible-light irradiation are shown in Figure 6. For reference, the result for no catalyst is also shown. From Figure 6, it is clear that the concentrations of RhB gradually decrease as a result of visible-light irradiation, whereas the concentration of RhB with no catalyst decreases negligibly. This phenomenon indicates that the degradation of the RhB solution is due to a photocatalytic reaction that happens upon irradiation by visible light. For $BiVO_4$ with 1% graphene, the photodegradation of RhB reaches 80% after 20 h of irradiation. For $BiVO_4$ with 0.25% graphene, the photodegradation of RhB reaches 87% after 20 h of irradiation, which demonstrates that the RhB molecules in solution have decomposed. In contrast, the photodegradation of RhB with pure $BiVO_4$ is 68% after irradiation for 20 h under the same conditions. The photodegradation of RhB with $BiVO_4$-graphene is more complete than that of pure $BiVO_4$, which is attributed to the graphene facilitating the transport of electrons photogenerated in the $BiVO_4$, thereby leading to an efficient separation of photogenerated carriers in the coupled $BiVO_4$-graphene system. The end result is an increase in photoconversion efficiency [14].

A possible reaction process is proposed in Figure 7. Upon visible-light excitation, electron-hole pairs are generated on the $BiVO_4$ surface (R1), followed by rapid transfer of photogenerated electrons to graphene sheets via a percolation mechanism (R2) [31]. Next, the negatively charged graphene sheets can activate O_2 to produce $O_2^{\bullet-}$ (R3), while the holes can react with H_2O to form $^{\bullet}OH$ (R4). Finally, the active species (holes, $^{\bullet}OH$ and $O_2^{\bullet-}$) oxidize the dye molecules adsorbed on the active sites of the $BiVO_4$-graphene nanocomposite photocatalyst (R5) [13, 14]. The entire sequence is summarized here:

$$BiVO_4 + h\nu \longrightarrow BiVO_4\,(h + e) \quad \text{(R1)}$$

$$BiVO_4\,(e) + \text{graphene} \longrightarrow BiVO_4 + \text{graphene}\,(e) \quad \text{(R2)}$$

$$\text{graphene}\,(e) + O_2 \longrightarrow O_2^{\bullet-} + \text{graphene} \quad \text{(R3)}$$

$$BiVO_4\,(h) + OH^- \longrightarrow BiVO_4 + {}^{\bullet}OH \quad \text{(R4)}$$

$$\begin{aligned} &BiVO_4\,(h) + {}^{\bullet}OH + O_2^{\bullet-} + \text{dyes} \\ &\longrightarrow \text{degradation products} \end{aligned} \quad \text{(R5)}$$

However, increasing the graphene content did not lead to an increase in the photocatalytic activity of composites,

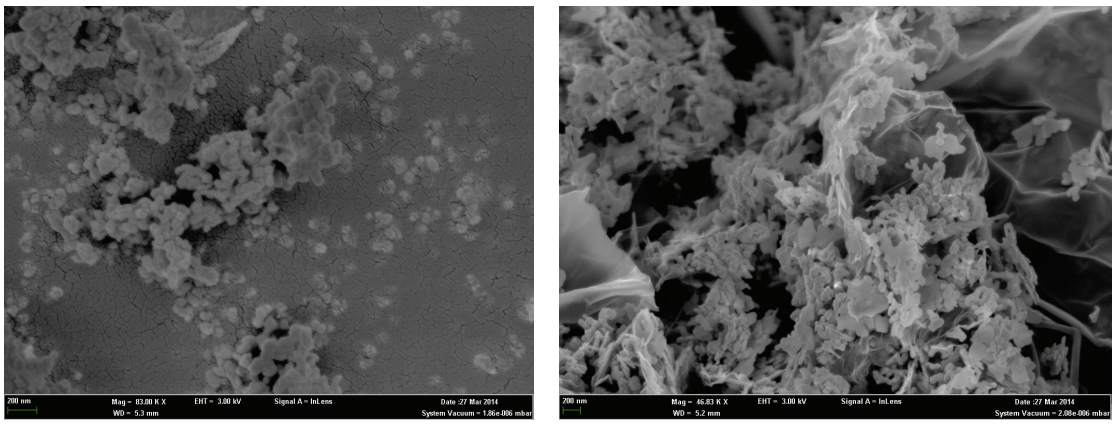

(a) $BiVO_4$ (b) $BiVO_4$-graphene

Figure 2: SEM images of pure $BiVO_4$ and $BiVO_4$-graphene catalyst.

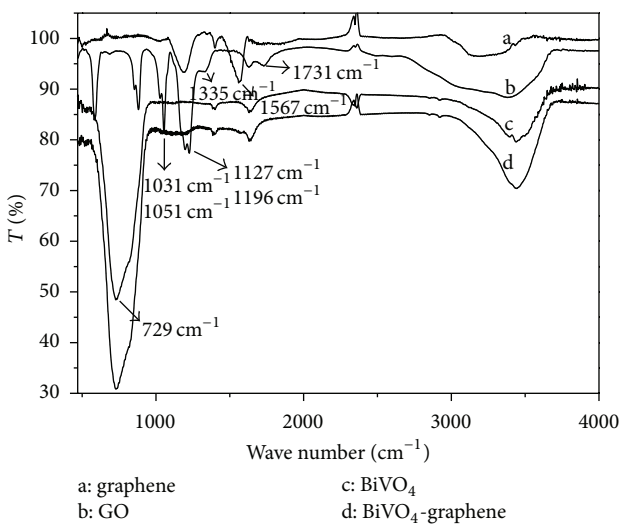

Figure 3: Fourier-transform infrared spectra of graphene, graphene oxide, pure $BiVO_4$, and $BiVO_4$-graphene composite.

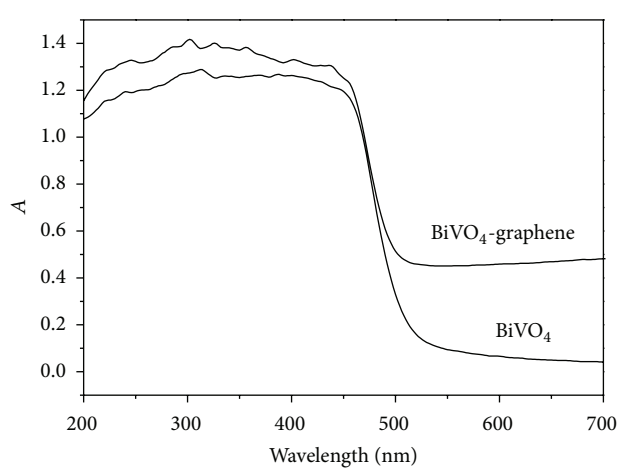

Figure 4: UV-visible absorption spectra of pure $BiVO_4$ and $BiVO_4$-graphene composite.

because too much graphene leads to the formation of recombination centers of electrons and holes. This parallel recombination pathway reduces the probability that photoexcited charges participate in the photocatalytic reaction. As a result, a high graphene content reduces the photocatalytic activity [32].

To study the contribution of electrons and holes to the degradation reaction, silver nitrate ($AgNO_3$, 0.2 mmol) and potassium sodium tartrate ($C_4H_4O_6KNa{\cdot}4H_2O$, 0.2 mmol) were added to the $BiVO_4$-graphene photocatalytic reaction system as electron-trapping agent and hole-trapping agent, respectively. This approach allows us to observe the degradation of RhB in the presence of either only electrons or only holes. As shown in Figure 8, adding silver nitrate clearly increases the degradation rate of RhB. In contrast, adding potassium sodium tartrate reduces the photocatalytic effect. These results suggest that the holes play the main role in the degradation of RhB in this system.

4. Conclusions

We prepared $BiVO_4$-graphene nanocomposites by using a facile single-step method and characterized the resulting samples by a variety of analytical methods. The results show that the graphene oxide in the catalyst is thoroughly reduced to graphene. In comparison with pure $BiVO_4$ catalyst, the synthesized nanocomposite catalyst is a more active photocatalyst for degrading rhodamine B dye under visible-light irradiation. We attribute the significant enhancement in photoactivity to the efficient separation of photogenerated carriers because of the high carrier mobility provided by graphene in the coupled $BiVO_4$-graphene system.

Conflict of Interests

The authors declare that there is no conflict of interests regarding the publication of this paper.

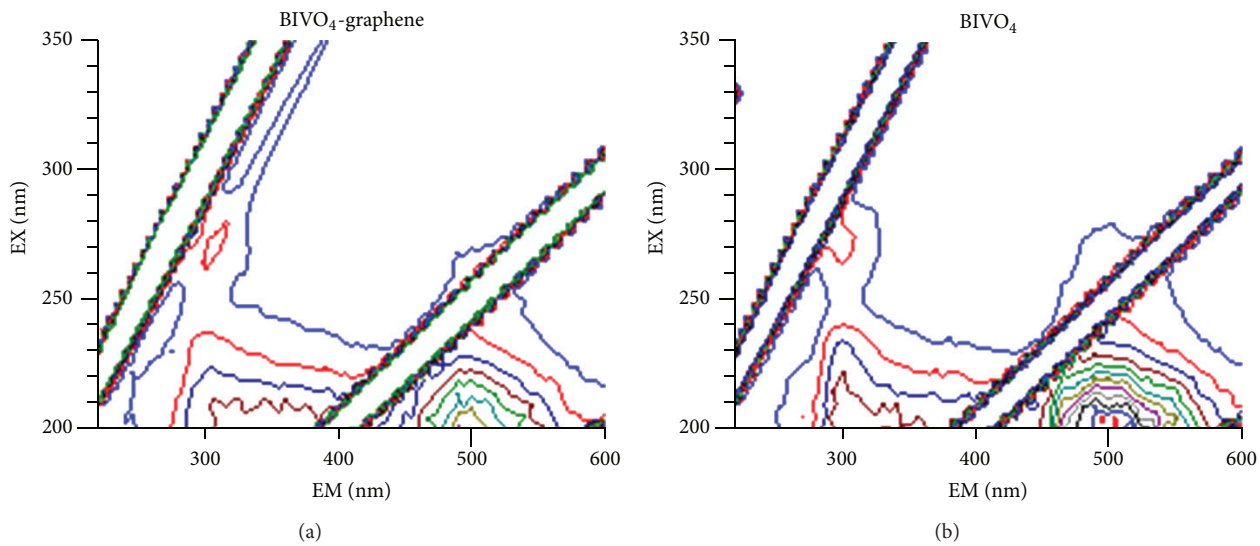

Figure 5: 3D fluorescence spectra of pure $BiVO_4$ and $BiVO_4$-graphene composite.

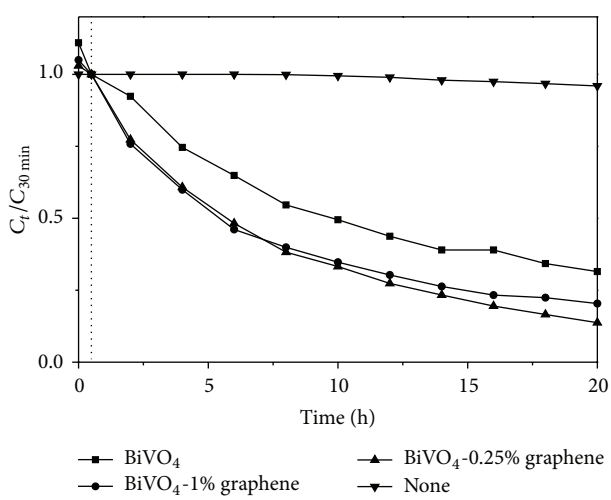

Figure 6: Concentration of RhB mixed with various photocatalysts (see legend) plotted as a function of time of exposure to visible-light irradiation. $C_{30\ \mathrm{min}}$ is the concentration of RhB after the reaction mixture was stirred for 30 min in the dark (to reach adsorption-desorption equilibrium between dye and the catalyst). C_t is the concentration of RhB after being irradiated by visible for time t.

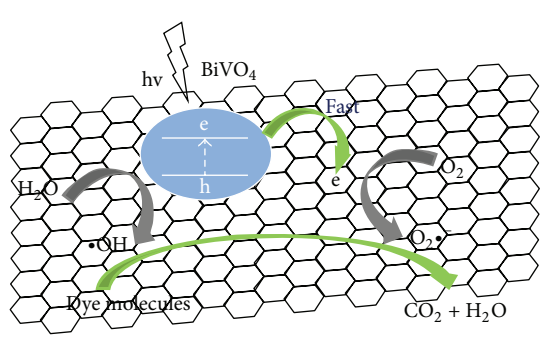

Figure 7: Photocatalytic reaction mechanism for $BiVO_4$-graphene composite.

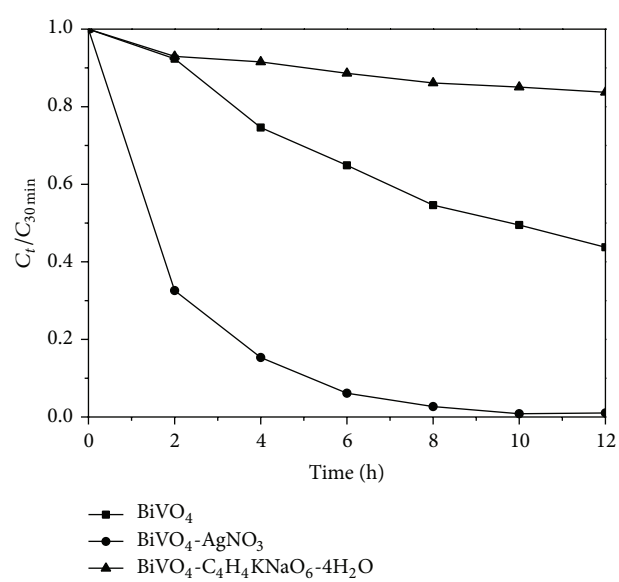

Figure 8: Photocatalytic degradation of RhB in $BiVO_4$-graphene after adding electron-trapping agent and hole-trapping agent.

Acknowledgments

The financial support of the National Natural Science Foundation of China (No. 51108483), the Natural Science Foundation Project of CQ CSTC (Grant No. cstcjjA20002), the 111 Project (No. B13041), and the Fundamental Research Funds for the Central Universities (CDJZR12210018, 106112013CDJZR210002) is gratefully acknowledged.

References

[1] Z. Zou, J. Ye, K. Sayama, and H. Arakawa, "Direct splitting of water under visible light irradiation with an oxide semiconductor photocatalyst," *Nature*, vol. 414, no. 6864, pp. 625–627, 2001.

[2] M. R. Hoffmann, S. T. Martin, W. Choi, and D. W. Bahnemann, "Environmental applications of semiconductor photocatalysis," *Chemical Reviews*, vol. 95, no. 1, pp. 69–96, 1995.

[3] M. Janus, J. Choina, and A. W. Morawski, "Azo dyes decomposition on new nitrogen-modified anatase TiO_2 with high adsorptivity," *Journal of Hazardous Materials*, vol. 166, no. 1, pp. 1–5, 2009.

[4] H. Fu, C. Pan, W. Yao, and Y. Zhu, "Visible-light-induced degradation of rhodamine B by nanosized Bi_2WO_6," *The Journal of Physical Chemistry B*, vol. 109, no. 47, pp. 22432–22439, 2005.

[5] A. Hernández, L. Maya, E. Sánchez-Mora, and E. M. Sánchez, "Sol-gel synthesis, characterization and photocatalytic activity of mixed oxide ZnO-Fe_2O_3," *Journal of Sol-Gel Science and Technology*, vol. 42, no. 1, pp. 71–78, 2007.

[6] Y. Sun, Y. Xie, C. Wu, S. Zhang, and S. Jiang, "Aqueous synthesis of mesostructured $BiVO_4$ quantum tubes with excellent dual response to visible light and temperature," *Nano Research*, vol. 3, no. 9, pp. 620–631, 2010.

[7] U. G. Akpan and B. H. Hameed, "The advancements in sol-gel method of doped-TiO_2 photocatalysts," *Applied Catalysis A: General*, vol. 375, no. 1, pp. 1–11, 2010.

[8] M. S. A. SherShah, K. Zhang, A. R. Park et al., "Single-step solvothermal synthesis of mesoporous Ag-TiO_2-reduced graphene oxide ternary composites with enhanced photocatalytic activity," *Nanoscale*, vol. 5, no. 11, pp. 5093–5101, 2013.

[9] A. Kudo, K. Omori, and H. Kato, "A novel aqueous process for preparation of crystal form-controlled and highly crystalline $BiVO_4$ powder from layered vanadates at room temperature and its photocatalytic and photophysical properties," *Journal of the American Chemical Society*, vol. 121, no. 49, pp. 11459–11467, 1999.

[10] K. Sayama, A. Nomura, T. Arai et al., "Photoelectrochemical decomposition of water into H_2 and O_2 on porous $BiVO_4$ thin-film electrodes under visible light and significant effect of Ag Ion treatment," *The Journal of Physical Chemistry B*, vol. 110, no. 23, pp. 11352–11360, 2006.

[11] A. Walsh, Y. Yan, M. N. Huda, M. M. Al-Jassim, and S.-H. Wei, "Band edge electronic structure of $BiVO_4$: elucidating the role of the Bi s and V d orbitals," *Chemistry of Materials*, vol. 21, no. 3, pp. 547–551, 2009.

[12] A. Mills and S. Le Hunte, "An overview of semiconductor photocatalysis," *Journal of Photochemistry and Photobiology A: Chemistry*, vol. 108, no. 1, pp. 1–35, 1997.

[13] Y. F. Sun, B. Y. Qu, Q. Liu et al., "Highly efficient visible-light-driven photocatalytic activities in synthetic ordered monoclinic $BiVO_4$ quantum tubes-graphene nanocomposites," *Nanoscale*, vol. 4, no. 12, pp. 3761–3767, 2012.

[14] Y. Fu, X. Sun, and X. Wang, "$BiVO_4$-graphene catalyst and its high photocatalytic performance under visible light irradiation," *Materials Chemistry and Physics*, vol. 131, no. 1-2, pp. 325–330, 2011.

[15] Y. Yan, S. F. Sun, Y. Song et al., "Microwave-assisted in situ synthesis of reduced graphene oxide-$BiVO_4$ composite photocatalysts and their enhanced photocatalytic performance for the degradation of ciprofloxacin," *Journal of Hazardous Materials*, vol. 250, pp. 1106–1114, 2013.

[16] M. Long, W. Cai, J. Cai, B. Zhou, X. Chai, and Y. Wu, "Efficient photocatalytic degradation of phenol over $Co_3O_4/BiVO_4$ composite under visible light irradiation," *The Journal of Physical Chemistry B*, vol. 110, no. 41, pp. 20211–20216, 2006.

[17] N. I. Kovtyukhova, P. J. Ollivier, B. R. Martin et al., "Layer-by-layer assembly of ultrathin composite films from micron-sized graphite oxide sheets and polycations," *Chemistry of Materials*, vol. 11, no. 3, pp. 771–778, 1999.

[18] Z. Fan, J. Yan, L. Zhi et al., "A three-dimensional carbon nanotube/graphene sandwich and its application as electrode in supercapacitors," *Advanced Materials*, vol. 22, no. 33, pp. 3723–3728, 2010.

[19] B. Cai, X. Y. Lv, S. Y. Gan et al., "Advanced visible-light-driven photocatalyst upon the incorporation of sulfonated graphene," *Nanoscale*, vol. 5, no. 5, pp. 1910–1916, 2013.

[20] H. Wang, L.-F. Cui, Y. Yang et al., "Mn_3O_4-graphene hybrid as a high-capacity anode material for lithium ion batteries," *Journal of the American Chemical Society*, vol. 132, no. 40, pp. 13978–13980, 2010.

[21] V. C. Tung, L.-M. Chen, M. J. Allen et al., "Low-temperature solution processing of graphene-carbon nanotube hybrid materials for high-performance transparent conductors," *Nano Letters*, vol. 9, no. 5, pp. 1949–1955, 2009.

[22] N. Zhang, Y. H. Zhang, and Y. J. Xu, "Recent progress on graphene-based photocatalysts: current status and future perspectives," *Nanoscale*, vol. 4, no. 19, pp. 5792–5813, 2012.

[23] C. Zhu, S. Guo, Y. Fang, and S. Dong, "Reducing sugar: new functional molecules for the green synthesis of graphene nanosheets," *ACS Nano*, vol. 4, no. 4, pp. 2429–2437, 2010.

[24] W. S. Hummers Jr. and R. E. Offeman, "Preparation of graphitic oxide," *Journal of the American Chemical Society*, vol. 80, no. 6, p. 1339, 1958.

[25] Y. H. Ng, A. Iwase, A. Kudo, and R. Amal, "Reducing graphene oxide on a visible-light $BiVO_4$ photocatalyst for an enhanced photoelectrochemical water splitting," *Journal of Physical Chemistry Letters*, vol. 1, no. 17, pp. 2607–2612, 2010.

[26] Y.-H. Yang, H.-J. Sun, T.-J. Peng, and Q. Huang, "Synthesis and structural characterization of graphene-based membranes," *Acta Physico: Chimica Sinica*, vol. 27, no. 3, pp. 736–742, 2011.

[27] W.-S. Ma, J.-W. Zhou, and S.-X. Cheng, "Preparation and characterization of graphene," *Journal of Chemical Engineering of Chinese Universities*, vol. 24, no. 4, pp. 719–722, 2010.

[28] J. Tang, Z. Zou, and J. Ye, "Photophysical and photocatalytic properties of $AgInW_2O_8$," *The Journal of Physical Chemistry B*, vol. 107, no. 51, pp. 14265–14269, 2003.

[29] G. Eda, Y.-Y. Lin, C. Mattevi et al., "Blue photoluminescence from chemically derived graphene oxide," *Advanced Materials*, vol. 22, no. 4, pp. 505–509, 2010.

[30] X. Xu, F.-Y. Ji, and L. He, "Structure and catalytic activity of CuO/TiO_2 modified by different kinds of surfactants," *Journal of Civil, Architectural and Environmental Engineering*, vol. 33, no. 1, pp. 129–134, 2011.

[31] X. Wang, L. J. Zhi, and K. Müllen, "Transparent, conductive graphene electrodes for dye-sensitized solar cells," *Nano Letters*, vol. 8, no. 1, pp. 323–327, 2008.

[32] X. Liu, L. Pan, T. Lv, G. Zhu, Z. Sun, and C. Sun, "Microwave-assisted synthesis of CdS-reduced graphene oxide composites for photocatalytic reduction of Cr(VI)," *Chemical Communications*, vol. 47, no. 43, pp. 11984–11986, 2011.